

Research paper

A recyclable cucurbit[6]uril-supported silicotungstic acid catalyst used in the esterification reaction



Wen Xia, Yu-Mei Nie, Na Lei, Zhu Tao, Qiang-Jiang Zhu, Yun-Qian Zhang*

Key Laboratory of Macrocyclic and Supramolecular Chemistry of Guizhou Province, Guizhou University, Guiyang 550025, China

ARTICLE INFO

Keywords:

Cucurbit[6]uril
Silicotungstic acid
Recyclable catalyst
Esterification reaction

ABSTRACT

The esterification reaction used to prepare butyl paraben (BP) and propyl gallate (PG) catalyzed using a cucurbit [6]uril-supported Keggin-type silicotungstic acid (Q[6]-STA) catalyst has been investigated. The Q[6]-STA catalyst has been characterized using FTIR spectroscopy, XRD, SEM, EDS, thermal analysis, and surface area studies. Q[6]-STA was easy to prepare in high yield and exhibited some advantageous properties, such as high catalytic activity and its convenient recovery. Moreover, a reusability study showed that the Q[6]-STA catalyst was stable and active.

1. Introduction

Heteropolyacids (HPAs), as a class of oxy acids, contain heteroatoms (such as P, Si, Fe and Co) and other metal atoms (such as Mo, W, V, Nb and Ta), which adopt certain structures based on their oxygen coordination [1]. HPAs with a Keggin-type structure are widely used as acid catalysts due to their novel structural properties and very strong Brønsted acidity [2]. Keggin-type HPAs, such as phosphomolybdic acid ($\text{H}_3\text{PMo}_{12}\text{O}_{40}$), silicotungstic acid ($\text{H}_4\text{SiW}_{12}\text{O}_{40}$) and phosphotungstic acid ($\text{H}_3\text{PW}_{12}\text{O}_{40}$), are readily available and most frequently used as acid catalysts [3]. However, the main disadvantages of using HPAs as catalysts are their relatively low surface area ($1\text{--}10\text{ m}^2\cdot\text{g}^{-1}$) and problematic separation from the reaction mixture [4,5].

Appending HPAs on a suitable support is expected to circumvent the above mentioned problems. As a result, many traditional acids have been immobilized on SiO_2 , Al_2O_3 , TiO_2 , active carbon, anion-exchange resin [6,7], clay [3], ZrO_2 [8] and Nb_2O_5 [9]. Cucurbit[*n*]urils (Q[*n*]s) are a family of host molecules possessing a rigid hydrophobic cavity and two identical carbonyl-fringed portals [10]. They have attracted a lot of attention in supramolecular chemistry because of their superior molecular recognition properties in aqueous media [11–25]. In particular, recently studies have revealed that the electrostatically positive outer surface of Q[*n*]s can provide a driving force, known as the outer-surface interaction of Q[*n*]s (OSIQ), which is capable of generating numerous novel Q[*n*]-based supramolecular assemblies, including Q[*n*]-HPA-based porous structures [26,27]. Kögerler and co-workers first investigated the interactions of $[\text{H}_2\text{O}@V^{IV}_{18}\text{O}_{42}]^{12-}$ with Q[6] and Q[8]

molecules, respectively and characterized two novel hybrid porous complexes [28]. Cao and co-workers prepared a series of hybrid Q[*n*]-HPA complexes [29–33] and demonstrated the photocatalytic activity of water-insoluble $\text{Q}[6]\text{--}[\text{SiW}_{12}\text{O}_{40}]^{4-}$ and $\text{Me}_{10}\text{Q}[5]\text{--}[\text{P}_2\text{W}_{18}\text{O}_{62}]^{6-}$ toward the degradation of methyl orange under visible light irradiation [34,35]. Ion-dipole interactions formed between the electrostatic potential positive outer surface of Q[*n*]s and HPAs anions, namely OSIQ [26,27], can adequately explain the formation of these water-insoluble materials. These results motivated our group to investigate Q[*n*]-supported HPAs as acid catalysts for the esterification reaction. In our previous work, tetramethyl cucurbit[6]uril-supported phosphomolybdic acid (TMeQ[6]-PMA) and perhydroxylated cucurbit[6]uril-supported phosphomolybdic acid $[(\text{HO})_{12}\text{Q}[6]\text{-PMA}]$ catalysts have been examined in the esterification reaction and showed good catalytic activity [36,37].

Butyl paraben (BP) and propyl gallate (PG) are commercially available products obtained from an esterification reaction. Some mineral acids, such as sulfuric and phosphoric acid, are conventionally used as catalysts for industrial scale esterification reactions. Although these mineral acid catalysts have many advantages, such as high catalytic activity and selectivity, they also have some disadvantages, such as being homogeneous reaction catalysts, difficult to recover, nonreusable, difficult to separate from the desired product, corrosive and toxic [38,39].

In this work, a cucurbit[6]uril-supported Keggin-type silicotungstic acid (Q[6]-STA) catalyst has been prepared, characterized and applied toward the synthesis of butyl paraben (BP) and propyl gallate (PG). The

* Corresponding author.

E-mail address: sci.yqzhang@gzu.edu.cn (Y.-Q. Zhang).

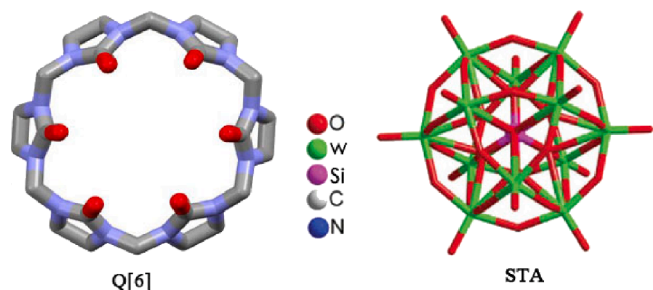


Fig. 1. Structure of cucurbit[6]uril (Q[6]) and silicotungstic acid (STA).

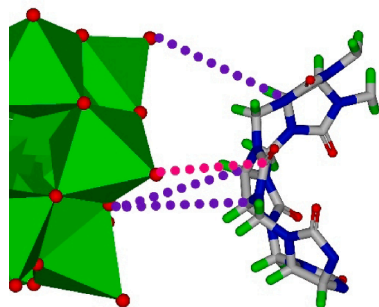


Fig. 2. The outer-surface interaction of Q[n] with HPAs.

structure of Q[6] and STA are shown in Fig. 1.

2. Experimental section

2.1. Materials

Reagent grade silicotungstic acid hydrate ($\text{H}_4\text{SiW}_{12}\text{O}_{40}\cdot x\text{H}_2\text{O}$; STA), p-hydroxybenzoic acid, gallic acid, butyl alcohol and propyl alcohol were purchased from Shanghai Aladdin Biochem Technology Co. Ltd. and used as received without further purification. Q[6] was synthesized according to a literature procedure [40].

2.2. Preparation of the Q[6]-STA catalyst

The Q[6]-STA catalyst was prepared by simply mixing solutions containing Q[6] and STA, respectively. A solution of STA ($2.5 \times 10^{-5} \text{ mol}\cdot\text{L}^{-1}$) in H_2O (10 mL) was added slowly to a solution of Q[6] ($5.0 \times 10^{-5} \text{ mol}\cdot\text{L}^{-1}$) in 3 M HCl (10 mL) with stirring. A precipitate immediately appeared and after stirring for a further 2 h, the solvent was removed under vacuum. The Q[6]-STA catalyst was dried at 353 K for 3 h to afford a yield of > 90% based on STA.

2.3. Characterization of the Q[6]-STA catalyst

The FTIR spectra of Q[6], STA and Q[6]-STA catalyst were measured on a Bruker Vertex 70 FTIR spectrometer using KBr pellets. Powder X-ray diffraction (XRD) analysis of Q[6]-STA was performed on a X'Pert-Pro MPD ($\text{CuK}\alpha$ radiation) and compared to mechanical mixtures of Q

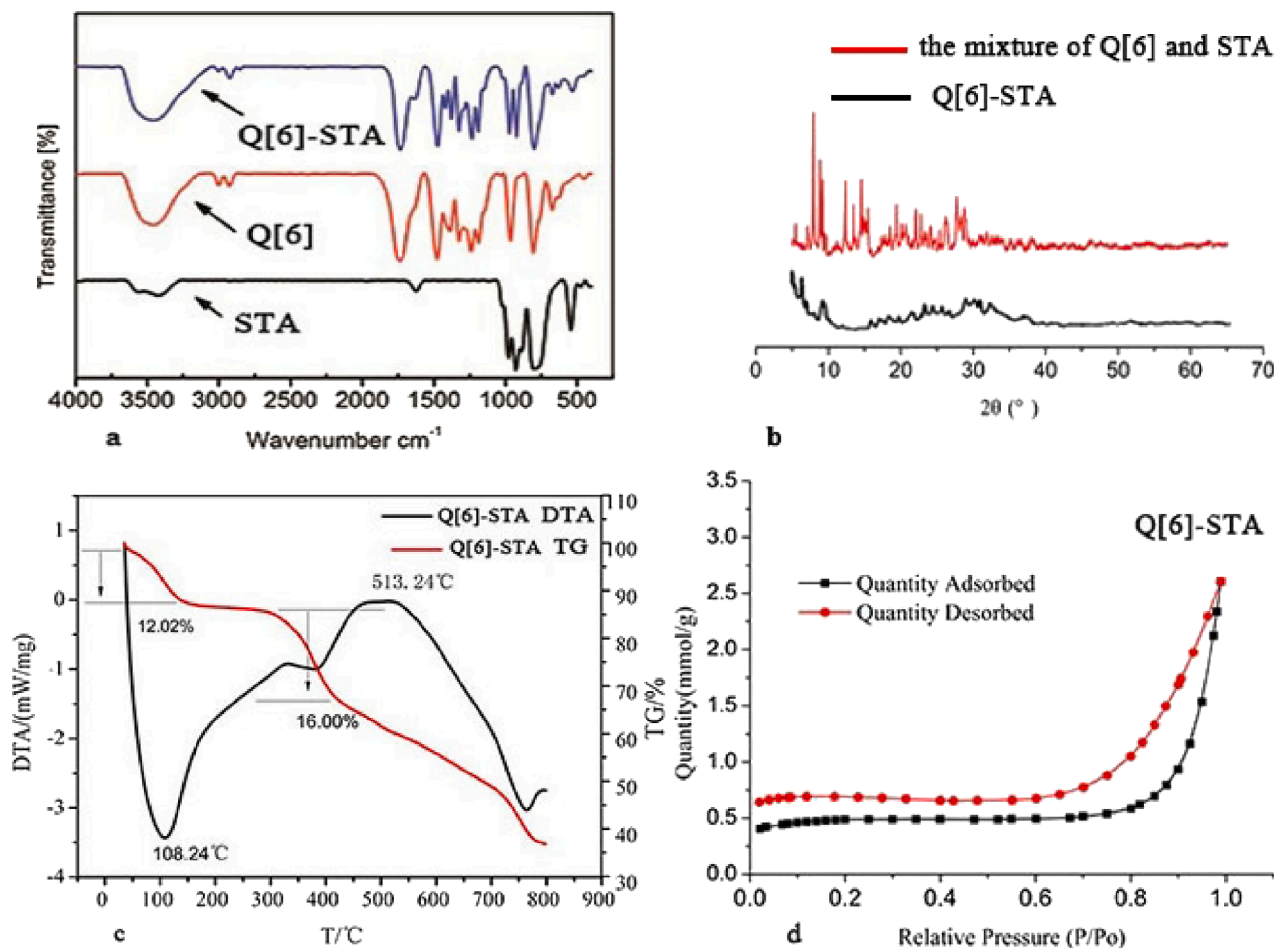


Fig. 3. (a) FTIR spectra obtained for Q[6], STA and the Q[6]-STA catalyst. (b) XRD patterns obtained for a simple mixture of Q[6] and STA, and the Q[6]-STA catalyst. (c) DTG and TG curves obtained for the Q[6]-STA catalyst. (d) Nitrogen gas adsorption-desorption isotherms obtained for the Q[6]-STA catalyst.

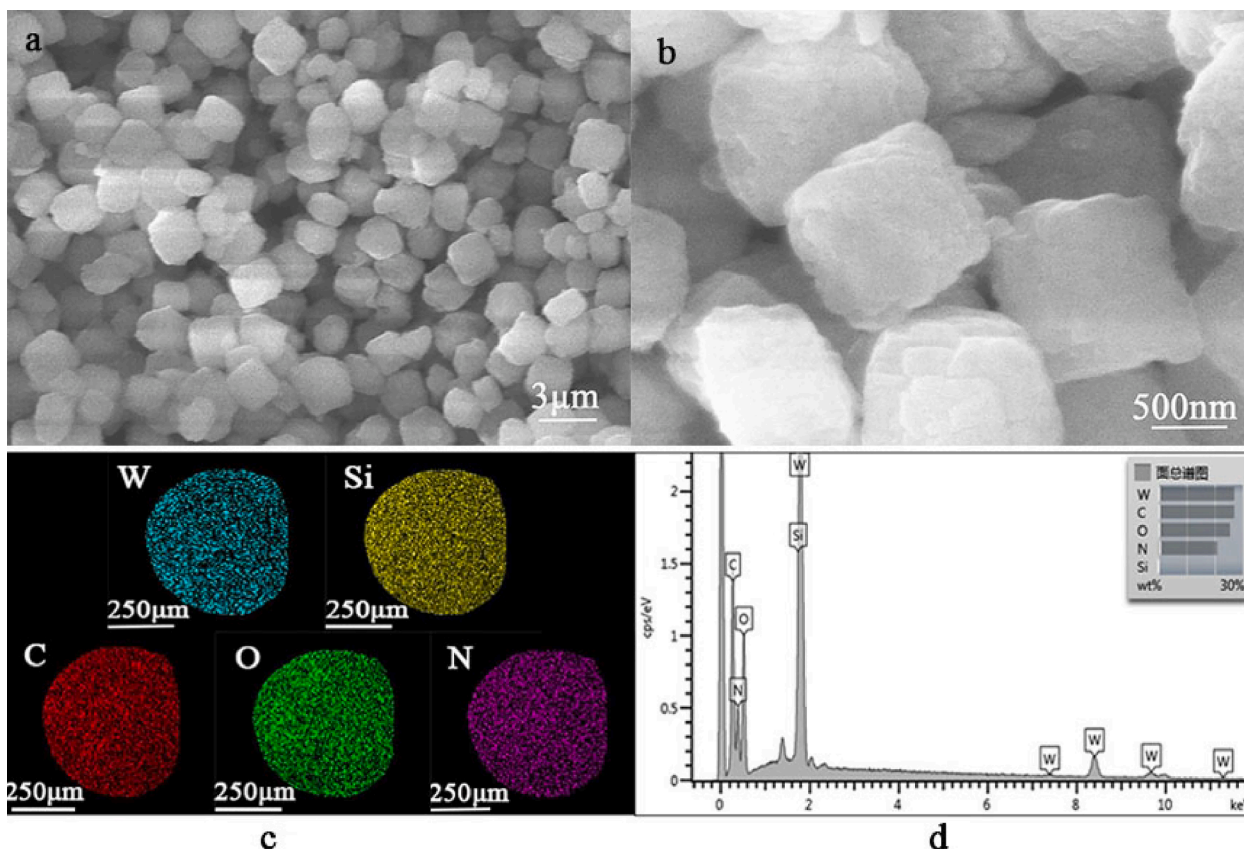


Fig. 4. (a,b) SEM images obtained for the Q[6]-STA catalyst. (c) The surface elemental analysis images and (d) corresponding composition of the Q[6]-STA catalyst obtained using EDS.

[6] and the STA. The XRD patterns of the samples were recorded in the 2θ range of $5 - 50^\circ$. TG-DTA analysis of the samples was carried out on an Netzsch STA499C thermal Analyzer using ~ 20 mg of sample in a platinum crucible. SEM and EDS were carried out using an Hitachi SU8010 FESEM instrument. The samples were suspended in ethanol, subjected to ultrasonication for 30 min, filtered and dried prior to measurement. The specific surface area, pore volume, and pore size distribution of the samples were measured on a ASAP 2020 HD88 automatic adsorption instrument using low temperature N_2 adsorption-desorption isotherms. Prior to measurement, the samples were degassed in situ at 393 K for 6 h under vacuum.

2.4. Catalytic tests

Q[6]-STA was used as a catalyst for the synthesis of butyl paraben (BP) to investigate its catalytic activity. 20–100 mg of freshly activated Q[6]-STA catalyst (dried at 353 K for 3 h), 0.036 mol of p-hydroxybenzoic acid and 0.072–0.432 mol of butyl alcohol were added to a 50-mL three-necked flask equipped with a reflux condenser and water separator, and the resulting reaction mixture was heated at reflux for 1–5 h. The resulting mixture was filtered while hot to separate the solid catalyst and the filtrate subjected to vacuum distillation to remove the excess butyl alcohol. The crude product was placed into a beaker, water added and the solution was left to stand at room temperature for 12 h. The resulting colorless crystals were filtered, washed with water ($3 \times$) and recrystallized from ethanol (75% v/v). The BP product was obtained via filtration, dried, weighed and the yield calculated.

In order to further investigate the catalytic performance of Q[6]-STA during the esterification reaction, PG was synthesized using a similar method to that used to prepare BP. A total of 20–150 mg of freshly activated Q[6]-STA catalyst (dried at 353 K for 3 h), 0.015 mol of gallate

acid, 0.015–0.210 mol of *n*-propyl alcohol and 5 mL of toluene as a water-carrying agent were added to a 50-mL three-necked flask equipped with a reflux condenser and water separator, and the resulting reaction mixture heated at reflux for 1–5 h. The resulting mixture was filtered while hot to separate the solid catalyst and the filtrate subjected to vacuum distillation to remove the excess *n*-propyl alcohol. The crude product was placed into a beaker, water added and the solution was left to stand at room temperature for 12 h. The resulting colorless crystals were filtered, washed with water ($3 \times$) and recrystallized from ethanol (75% v/v) to give PG.

The Q[6]-STA catalyst was recovered by filtration, washed with water, and vacuum-dried. The activated catalyst was reused for further experiments.

3. Results and discussion

3.1. Interaction of Q[6] and HPA

It is common that Q[n]s interact with HPAs in aqueous media to form water-insoluble hybrid compounds, in which the driving force is derived from the so-called OSIQ[26]. That is to say, the electrostatically positive outer surface of the Q[n] interacts with the HPAs anions via ion-dipole interactions, which generally involve the protruding oxygen atoms of the HPAs and portal carbonyl carbon atoms or methine/methylene protons on the back of the Q[n] (Fig. 2) [28]. Previous studies have revealed that some Q[n]s interact with selected HPAs to form hybrid compounds via OSIQ[23,28–35]. Generally, Q[n] molecules interact with HPAs in simple ratios, such as 1:1 [28,31,33,34] or 2:1 [29,30,32,33,35]. This was corroborated in the present work when we prepared a Q[6]-supported STA catalyst. The as-obtained precipitate exhibited a fixed composition and was obtained in high yield (>90%

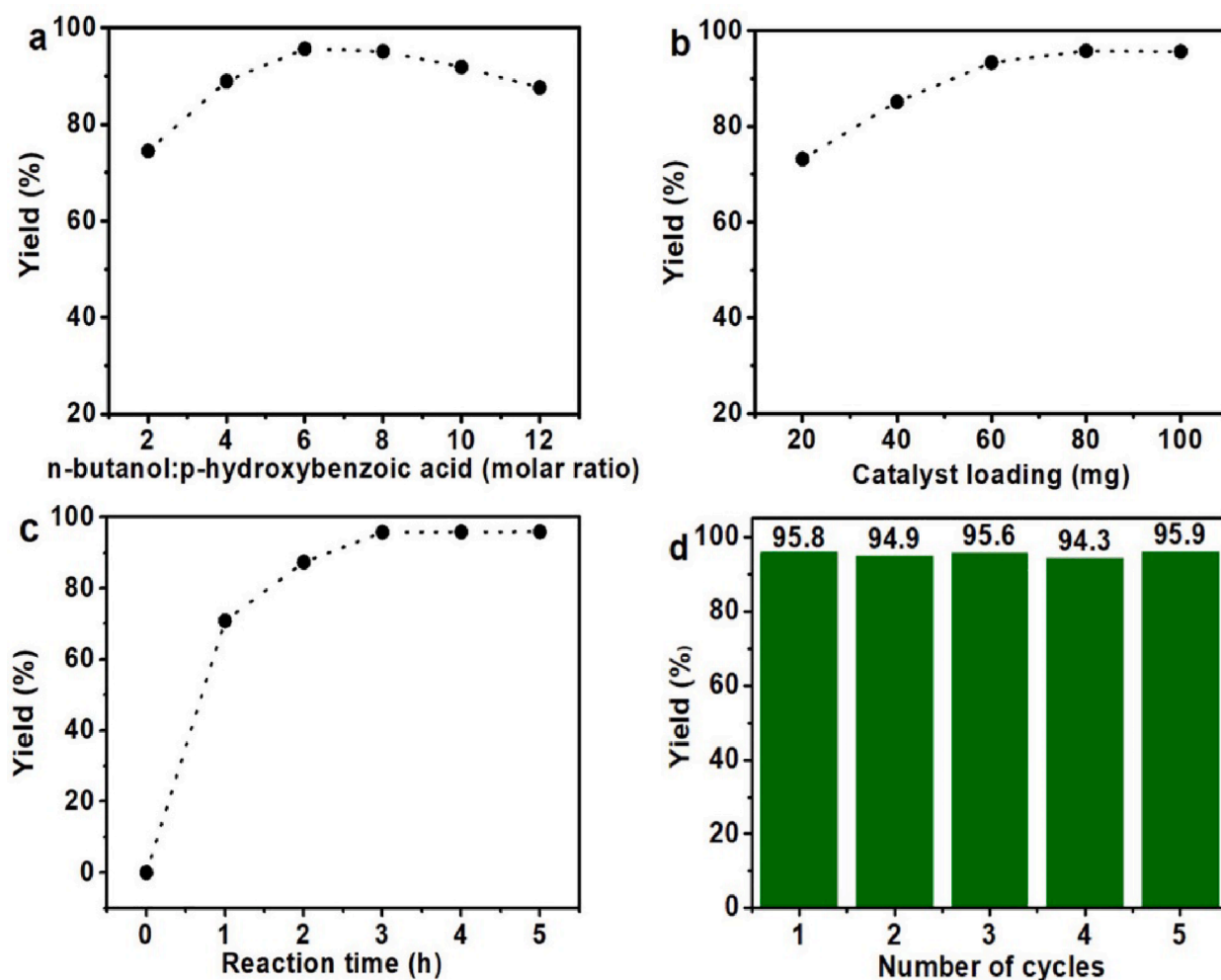


Fig. 5. (a) The influence of the molar ratio of the reactants on the yield of BP. (b) The influence of the catalyst loading on the yield of BP. (c) The influence of the reaction time on the yield of BP. (d) The synthesis of BP was repeated 5 times under the optimal reaction conditions.

based on STA). The elemental analysis results showed that the Q[6]:STA stoichiometry was consistently 2:1 and the chemical formula was $C_{72}H_{76}N_{48}O_{64}SiW_{12} \cdot nH_2O$.

3.2. Characterization of the Q[6]-STA catalyst

Fourier-transform infrared (FTIR) spectroscopy provides an insight into the interaction of Q[6] with STA (Fig. 3a). Generally, Q[6] exhibits characteristic IR bands at 2929 cm^{-1} [$\nu(-CH_2-)$] and 1728 cm^{-1} (terminal C=O). Meanwhile, STA exhibits four characteristic IR bands at 1080 cm^{-1} (Si-O in central tetrahedron), 980 cm^{-1} (terminal W=O), 890 cm^{-1} (corner-sharing oxygen), and 800 cm^{-1} (W-O-W edge-sharing bridging oxygen) [1]. When compared to the spectra obtained for the two pure compounds (Q[6] and STA), the characteristic IR bands of Q[6] and STA can still be observed in the Q[6]-STA catalyst. In particular, the bands due to the portal carbonyl groups showed no obvious changes, whereas the bands due to the bridging $-CH_2-$ showed different shapes, suggesting that the STA molecules may reside on the outer surface via weak intermolecular interactions. It is conceivable that the electrostatically negative carbonyl-fringed portals of the Q[6] molecules may prevent the approach of the STA anions. Evidently, Q[6] and STA maintained their initial structures in the Q[6]-STA catalyst without being destroyed. The XRD patterns of Q[6]-STA was completely different from that of a simple mixture of Q[6] and STA (Fig. 3b), indicating that a new phase was formed between Q[6] and STA in solution, that is, Q[6] formed interactions with STA. Thermogravimetric

analysis was carried out on the Q[6]-STA catalyst (Fig. 3c), which showed a mass loss of 12.02% at $108.24\text{ }^\circ\text{C}$. This can be attributed to the loss of free water from the compound. The following two endothermic bands corresponded to decomposition of Q[6] and STA at $378.74\text{ }^\circ\text{C}$ and $760\text{ }^\circ\text{C}$. These experimental results suggested that the interactions formed between STA and Q[6] render STA with increased thermal stability. Nitrogen gas adsorption measurements were applied to characterize the porosity of the Q[6]-STA catalyst (Fig. 3d). The surface area was calculated from the isotherms using the multi-point Brunauer-Emmett-Teller (BET) method. The pore size distribution was determined using the Barrett-Joyner-Halenda (BJH) method from the desorption parts of the isotherms. The results showed that the BET surface area, micropore volume and pore size of the Q[6]-STA catalyst were $55.41\text{ m}^2 \cdot \text{g}^{-1}$, $0.018\text{ cm}^3 \cdot \text{g}^{-1}$ and 27.66 nm , respectively. Evidently, the surface area of the Q[6]-supported STA was greater than that of the unsupported STA [4,5].

The morphologies and elemental distribution of the Q[6]-STA catalyst were investigated using SEM and EDS. The SEM image shows that the Q[6]-STA catalyst was uniform with a particle size of $\sim 100\text{ nm}$ (Fig. 4a,b) and the surface of the composite was rough, which was beneficial for the enhanced contact area between the catalyst and reactant. Furthermore, the surface elemental analysis (Fig. 4c) and strong peaks attributed to C, N, O, Si and W were observed in the EDS spectrum (Fig. 4d), and confirmed that the composition of the sample was consistent with the Q[6]-STA catalyst.

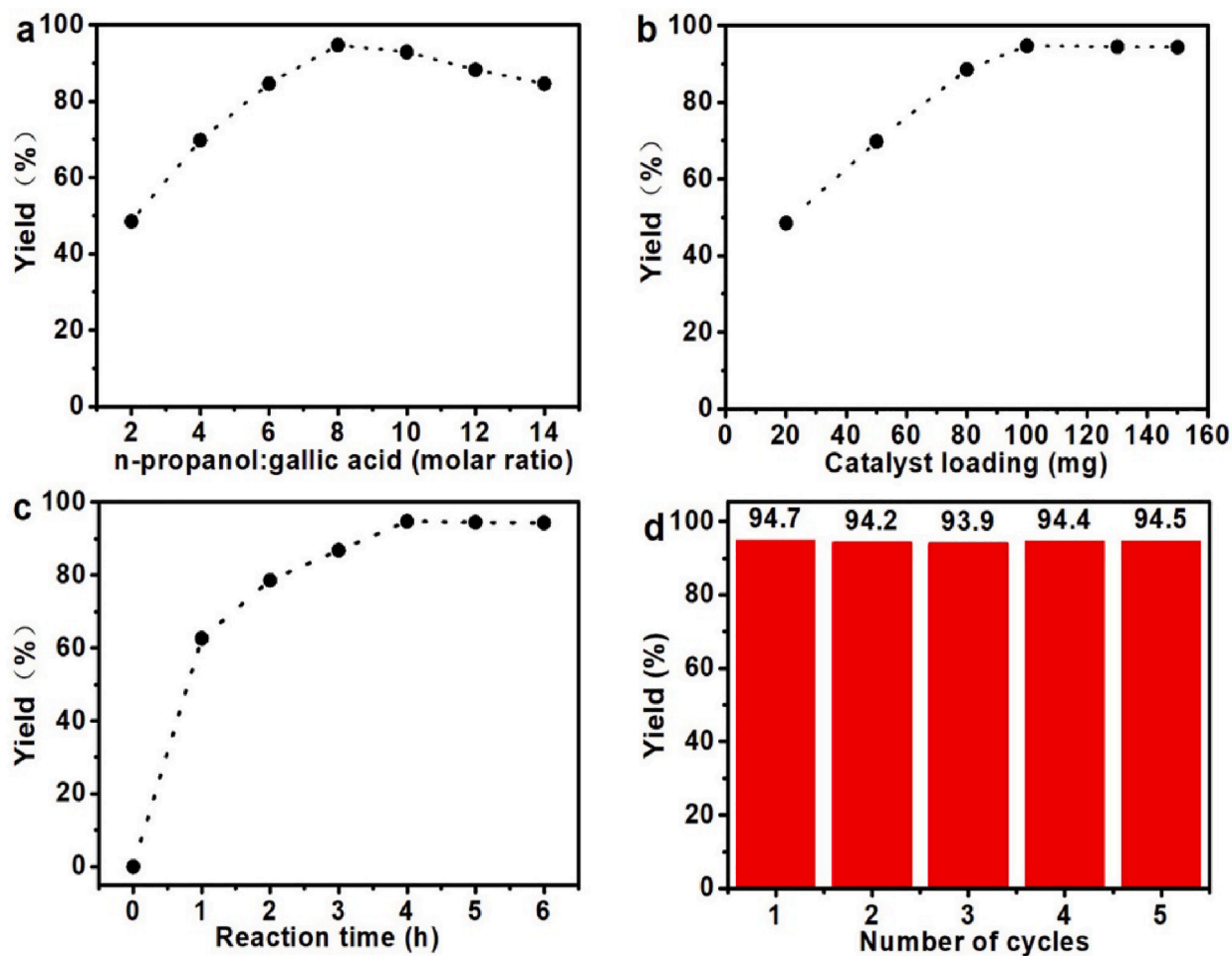


Fig. 6. (a) Influence of the molar ratio of the reactants on the yield of PG. (b) The influence of the catalyst loading on the yield of PG. (c) The influences of the reaction time on the yield of PG. (d) The synthesis of PG was repeated five times under the optimal reaction conditions.

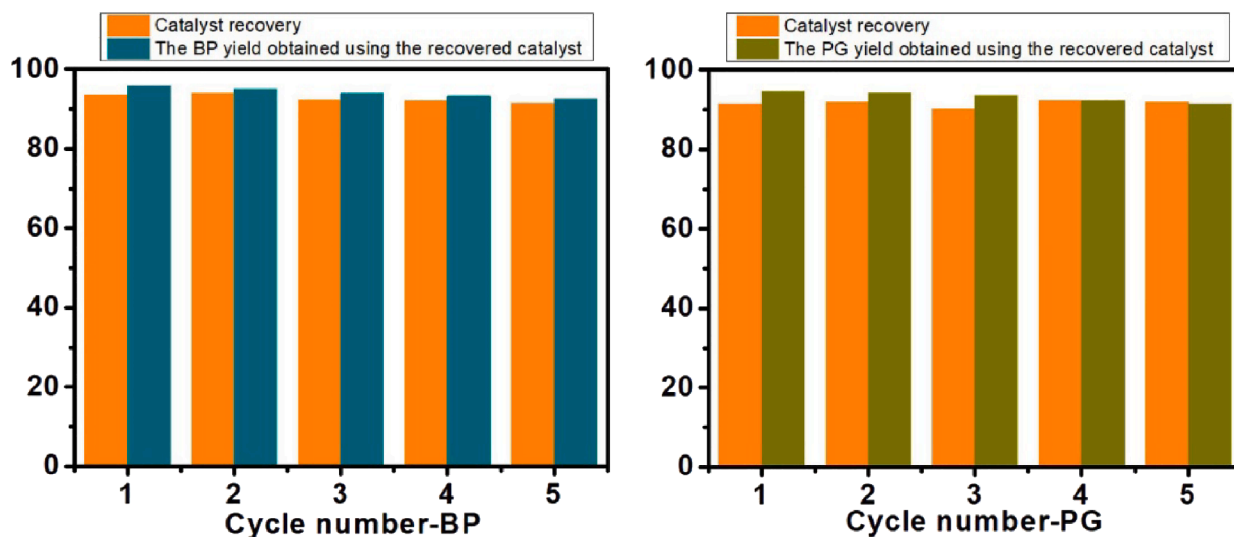


Fig. 7. The reusability of the Q[6]-STA catalyst in the esterification reaction used to prepare BP and PG.

3.3. Catalytic activity tests using the Q[6]-STA catalyst

In order to evaluate the catalytic activity of the Q[6]-supported STA catalyst, it was applied in the esterification reaction. The influencing

factors, including catalyst loading, reaction time and molar ratio of acid to alcohol, on the synthesis of BP and PG were investigated. BP was synthesized heating different molar ratios of butyl alcohol to p-hydroxybenzoic acid with 100 mg Q[6]-STA catalyst at reflux for 3 h

(Fig. 5a). The optimal molar ratio of butyl alcohol to p-hydroxybenzoic acid was identified to be 6:1, which gave the maximum yield of BP (95.6%). Fig. 5b shows the influence of the catalyst loading on the yield of BP using a fixed molar ratio of butyl alcohol to p-hydroxybenzoic acid of 6:1 at reflux for 3 h. The yield of BP increased upon increasing the catalyst loading with a maximum yield of 95.8% obtained when using 80 mg of the Q[6]-STA catalyst. To investigate the influence of reaction time on the yield of BP, the molar ratio of butyl alcohol to p-hydroxybenzoic acid was fixed at 6:1, the catalyst loading was fixed at 80 mg and the reaction heated at reflux. Fig. 5c shows the yield of BP increased upon increasing the reaction time up to 3 h, after which it levelled off at 95.8%. Under optimal conditions (catalyst loading, 80 mg; molar ratio of butyl alcohol to p-hydroxybenzoic, 6:1; reaction temperature, 391 K, reaction time, 3 h), the reaction was repeated 5 times. The results showed that the yield of BP was maintained at ~95% (Fig. 5d).

In the PG synthesis, the reaction conditions were similar to that used to prepare BP and the details listed in Table S1–S4. The optimum reaction conditions were catalyst loading, 100 mg; molar ratio of *n*-propanol to gallic acid, 8:1; reaction temperature, 370 K; reaction time, 4 h. The yield of PG was >94% over five repeated reactions (Fig. 6). BP and PG were characterized using FTIR and NMR spectroscopy, and the results shown in Figs. S1 and S2.

Q[6] has no catalytic activity in esterification reaction, and its role is to form a stable solid catalyst through the self-assembly interaction of Q[6] and STA. The active species in Q[6]-STA is STA. However, control experiments revealed the low efficiency of unsupported STA. When 47 mg of STA was used as a homogeneous catalyst, the yield of BP was found to be 85%. And the yield of PG became as low as 83% using 59 mg of pristine STA. The results showed that the catalytic performance of Q[6]-STA is better than that of unsupported STA.

Q[n]-HPAs self-assembled systems often have the characteristics of porous structure [28,36]. In addition, the morphology of Q[6]-STA nanoparticles also increase its surface area and active site on the catalyst surface. The greater the specific surface area of the catalyst, the more dispersed the active species, and the larger the number of active sites. The high porosity of the catalyst makes it easy to adsorb the reactants, thus enhancing its catalytic performance.

Since STA is a Brønsted acid [2,41], we speculate that the aforementioned reaction can be explained by acid-catalysed Fischer esterification mechanism [42]. When the carbonyl oxygen atom of carboxylic group binds with a proton of STA, the density of positive charge on carbonyl carbon atom increases. The nucleophilic attack of the alcohol on the protonated carbonyl group gives a tetrahedral intermediate bearing two hydroxyl groups, which undergoes a water and proton elimination process to produce the ester.

3.4. Recyclability of the Q[6]-HPA catalyst.

We previously mentioned that the Q[6]-STA catalyst can be easily prepared in high yield and shows high stability because it is insoluble in both acidic aqueous solutions and organic solvents. As an esterification reaction catalyst, Q[6] – STA is characterized by its high catalytic activity when compared to its classical counterparts and it may be easily isolated from reaction media via filtration due to its insolubility. An additional important advantage of the Q[6]-STA catalyst is its stability with respect to leaching of the acid sites during the esterification reaction. Thus, the catalyst can be collected using simple filtration after completion of the reaction. The catalyst can be regenerated by washing with water several times, followed by drying at 373 K in an oven under an air atmosphere. Thereafter, it can be reused in a new esterification reaction system. Fig. 7 shows the results of 5 consecutive reactions under the optimal conditions used to prepare BP and PG with the Q[6]-STA catalyst. The normalized yields suggested the catalyst retained its original catalytic activity. XRD shows that the composition and structure of Q[6]-STA remained unchanged after repeated use (Fig. S3).

4. Conclusion

In this work, a cucurbit[6]uril-supported silicotungstic acid (Q[6]-STA) catalyst has been prepared. Q[6] and STA not only exhibited good catalytic activity in the esterification reaction, but are also insoluble solids, which could be easily isolated from the reaction system. The Q[6]-supported STA enhanced the stability of STA and improved its catalytic efficiency.

CRedit authorship contribution statement

Wen Xia: Conceptualization, Investigation, Writing - original draft. **Yu-Mei Nie:** Investigation. **Na Lei:** Investigation. **Zhu Tao:** Resources. **Qiang-Jiang Zhu:** Resources. **Yun-Qian Zhang:** Resources, Conceptualization, Supervision.

Declaration of Competing Interest

The authors declare that they have no known competing financial interests or personal relationships that could have appeared to influence the work reported in this paper.

Acknowledgements

We acknowledge the support of the National Natural Science Foundation of China (No. 21761007, 21871064).

Appendix A. Supplementary data

Supplementary data to this article can be found online at <https://doi.org/10.1016/j.ica.2021.120418>.

References

- [1] E.B. Wang, C.W. Hu, L. Xu, *Introduce in Polyacid Chemistry (in Chinese)*, Chemical Industry Press, Beijing, 1997, p. 4.
- [2] J. Haber, K. Pamin, L. Matachowski, D. Mucha, *Appl. Catal. A* 256 (2003) 141–152, [https://doi.org/10.1016/S0926-860X\(03\)00395-8](https://doi.org/10.1016/S0926-860X(03)00395-8).
- [3] S.K. Bhorodwaj, D.K. Dutta, *Appl. Clay Sci.* 53 (2011) 347–352, <https://doi.org/10.1016/j.clay.2011.01.019>.
- [4] D.P. Sawant, A. Vinu, J. Justus, P. Srinivasu, S.B. Halligudi, *J. Mol. Catal. A: Chem.* 276 (2007) 150–157, <https://doi.org/10.1016/j.molcata.2007.07.001>.
- [5] M.N. Timofeeva, M.M. Matrosova, T.V. Reshetenko, L.B. Avdeeva, A.A. Budneva, A.B. Ayupov, E.A. Paukshtis, A.L. Chuvilin, A.V. Volodin, V.A. Likhobov, *J. Mol. Catal. A: Chem.* 211 (2004) 131–137, <https://doi.org/10.1016/j.molcata.2003.10.019>.
- [6] Y. Wu, X.K. Ye, X.G. Yang, X.P. Wang, W.L. Chu, Y.C. Hu, *Ind. Eng. Chem. Res.* 35 (1996) 2546–2560, <https://doi.org/10.1021/ie950473s>.
- [7] R.M. Ladera, M. Ojeda, J.L.G. Fierro, S. Rojas, *Catal. Sci. Technol.* 5 (2015) 484–491, <https://doi.org/10.1039/C4CY00998C>.
- [8] J.G. Hernández-Corteza, M.a. Manríquez, L. Lartundo-Rojas, E. López-Salinas, *Catalysis Today* 220–222 (2014) 32–38, <https://doi.org/10.1016/j.cattod.2013.09.007>.
- [9] S. An, D.Y. Song, Y.N. Sun, Y.H. Guo, Q.K. Shang, *Microporous Mesoporous Mater.* 226 (2016) 396–405, <https://doi.org/10.1016/j.jcat.2016.07.004>.
- [10] H. Cong, X.L. Ni, X. Xiao, Y. Huang, Q.J. Zhu, S.F. Xue, Z. Tao, L.F. Lindoy, G. Wei, *Org. Bio Mol. Chem.* 14 (2016) 4335, <https://doi.org/10.1039/c6ob00268d>.
- [11] J.W. Lee, S. Samal, N. Selvapalam, H.J. Kim, K. Kim, *Acc. Chem. Res.* 36 (2003) 621, <https://doi.org/10.1002/chin.2003046280>.
- [12] K. Kim, *Chem. Soc. Rev.* 31 (2002) 96, <https://doi.org/10.1039/a900939f>.
- [13] J. Lagona, P. Mukhopadhyay, S. Chakrabarti, L. Isaacs, *Angew. Chem. Int. Ed.* 44 (2005) 4844, <https://doi.org/10.1002/anie.200460675>.
- [14] K. Kim, N. Selvapalam, Y.H. Ko, K.M. Park, D. Kim, J. Kim, *Chem. Soc. Rev.* 36 (2007) 267, <https://doi.org/10.1039/b603088m>.
- [15] R.N. Souza, U. Pischel, W.M. Nau, *Chem. Rev.* 111 (2011) 7941, <https://doi.org/10.1021/cr200213s>.
- [16] V. Sindelar, S. Silvi, S.E. Parker, D. Sobransingh, A.E. Kaifer, *Adv. Funct. Mater.* 17 (2007) 694, <https://doi.org/10.1002/adfm.200600969>.
- [17] S. Gadde, A.E. Kaifer, *Cur. Org. Chem.* 15 (2011) 27, <https://doi.org/10.2174/138527211793797800>.
- [18] L. Isaacs, *Acc. Chem. Res.* 47 (2014) 2052, <https://doi.org/10.1021/ar500075g>.
- [19] K.I. Assaf, W.M. Nau, *Chem. Soc. Rev.* 44 (2015) 394, <https://doi.org/10.1039/c4cs00273c>.
- [20] M.N. Sokolov, D.N. Dybtsev, V.P. Fedin, *Russ. Chem. Bull., Int. Ed.* 52 (2003) 1041, <https://doi.org/10.1023/A:1024771902420>.

- [21] O.A. Gerasko, M.N. Sokolov, V.P. Fedin, *Pure Appl. Chem.* 76 (2004) 1633, <https://doi.org/10.1351/pac200476091633>.
- [22] V.P. Fedin, J. Russ, *Coordin. Chem.* 30 (2004) 151, <https://doi.org/10.1023/B:RUCO.0000022114.76939.16>.
- [23] J. Lü, J.X. Lin, M.N. Cao, R. Cao, *Coord. Chem. Rev.* 257 (2013) 1334, <https://doi.org/10.1016/j.ccr.2012.12.014>.
- [24] X.L. Ni, X. Xiao, H. Cong, L.L. Liang, K. Chen, X.J. Cheng, N.N. Ji, Q.J. Zhu, S. F. Xue, Z. Tao, *Chem. Soc. Rev.* 42 (2013) 9480, <https://doi.org/10.1039/c3cs60261c>.
- [25] X.L. Ni, S.F. Xue, Z. Tao, Q.J. Zhu, L.F. Lindoy, G. Wei, *Coord. Chem. Rev.* 287 (2015) 89, <https://doi.org/10.1016/j.ccr.2014.12.018>.
- [26] X.L. Ni, X. Xiao, H. Cong, Q.J. Zhu, S.F. Xue, Z. Tao, *Acc. Chem. Res.* 47 (2014) 1386, <https://doi.org/10.1021/ar5000133>.
- [27] Y. Huang, R.H. Gao, X.L. Ni, X. Xiao, H. Cong, Q.J. Zhu, K. Chen, Z. Tao, Preprint at, *Angew. Chem. Int. Ed.* (2020), <https://doi.org/10.1002/anie.202002666>.
- [28] X.K. Fang, P. Kogerler, L. Isaacs, S. Uchida, N. Mizuno, *J. Am. Chem. Soc.* 131 (2009) 432, <https://doi.org/10.1021/ja807751b>.
- [29] J.X. Lin, J. Lu, R. Cao, J.T. Chen, C.Y. Su, *Dalton Trans.* (2009) 1101–1103, <https://doi.org/10.1039/B817537N>.
- [30] J.X. Lin, J. Lu, H.X. Yang, R. Cao, *Cryst. Growth Des.* 2010 (1966) 10, <https://doi.org/10.1021/cg1000528>.
- [31] J.X. Lin, J. Lu, M.N. Cao, R. Cao, *Cryst. Growth Des.* 11 (2011) 778, <https://doi.org/10.1021/cg101355d>.
- [32] L.W. Han, J. Lu, X.J. Lin, R. Cao, *Dalton Trans.* 41 (2012) 10080, <https://doi.org/10.1039/c2dt30559c>.
- [33] N.C. Kasuga, M. Umeda, H. Kidokoro, K. Ueda, K. Hattori, K. Yamaguchi, *Cryst. Growth Des.* 9 (2009) 1494, <https://doi.org/10.1021/cg801007k>.
- [34] M. Cao, J. Lin, X.J. Lu, Y. You, T. Liu, R. Cao, *J. Hazard. Mater.* 186 (2011) 948, <https://doi.org/10.1016/j.jhazmat.2010.10.119>.
- [35] J. Lu, J.X. Lin, X.L. Zhao, R. Cao, *Chem. Commun.* 48 (2012) 669, <https://doi.org/10.1039/c1cc16268c>.
- [36] X. Xia, W.W. Ge, H.Y. Chen, Z. Tao, Y.Q. Zhang, G. Wei, K. Chen, *New J. Chem.* 43 (2019) 10297–10304, <https://doi.org/10.1039/C9NJ01116A>.
- [37] S. Li, W. Xia, Y.Q. Zhang, Z. Tao, *New J. Chem.* 44 (2020) 11895–11900.
- [38] T.A. Peters, N.E. Benes, A. Holmen, J.T.F. Keurentjes, *Appl. Catal. A* 297 (2006) 182–188, <https://doi.org/10.1016/j.apcata.2005.09.006>.
- [39] J.A. Dias, E. Caliman, S.C.L. Dias, M. Paulo, A.T.C.P. de Souza, *Catal. Today* 85 (2003) 39–48, [https://doi.org/10.1016/S0920-5861\(03\)00192-5](https://doi.org/10.1016/S0920-5861(03)00192-5).
- [40] W.A. Freeman, W.L. Mock, N.Y. Shih, Cucurbituril, *J. Am. Chem. Soc.* 103 (1981) 7367, <https://doi.org/10.1021/ja00414a070>.
- [41] M.N. Timofeeva, *Appl. Catal. A: Gen.* 256 (2003) 19, [https://doi.org/10.1016/S0926-860X\(03\)00386-7](https://doi.org/10.1016/S0926-860X(03)00386-7).
- [42] C.B. Vilanculo, L.C.A. Leles, M.J. Silva, *Waste Biomass Valorization* 2020 (1895) 11, <https://doi.org/10.1007/s12649-018-00549-x>.